Applied Physics Letters

High photoresponse inverted ultraviolet photodetectors consisting of iridium phosphor doped into poly(N-vinylcarbazole) polymeric matrix

Cite as: Appl. Phys. Lett. **104**, 173304 (2014); https://doi.org/10.1063/1.4874610
Submitted: 17 January 2014 . Accepted: 21 April 2014 . Published Online: 01 May 2014

Xiao Wang, Jiang Huang, Shijiao Han, and Junsheng Yu

High photoresponse inverted ultraviolet photodectectors consisting of iridium phosphor doped into poly(N-vinylcarbazole) polymeric matrix

Xiao Wang, Jiang Huang, Shijiao Han, and Junsheng Yu[a)]
State Key Laboratory of Electronic Thin Films and Integrated Devices, School of Optoelectronic Information, University of Electronic Science and Technology of China (UESTC), Chengdu 610054, People's Republic of China

(Received 17 January 2014; accepted 21 April 2014; published online 1 May 2014)

Highly sensitive inverted polymer ultraviolet (UV) photodectectors were fabricated by doping a phosphorescent material of bis[2-(4-tertbutylphenyl)benzothiazolato-N,C2′] iridium(acetylacetonate) [$(t\text{-}bt)_2Ir(acac)$] into poly(N-vinylcarbazole) (PVK) polymeric matrix. Under the UV-260 nm illumination with an intensity of 0.7 mW/cm^2, the device achieved a photocurrent of 11.37 mA/cm^2 at −3 V, corresponding to a photoresponse of 15.97 A/W, which is 381% higher than the undoped device. Detailed analysis of photoluminescence, charge carrier transportation and film morphologies of PVK polymer active layers were carried out, and the enhanced UV absorption, formation of the triplet excitons and better charge carrier transport are ascribed to the improved photodectector performance. © *2014 AIP Publishing LLC*. [http://dx.doi.org/10.1063/1.4874610]

Recently, ultraviolet photodetectors (UV-PDs) are drawing considerable attention owing to their wide application in fields like solar astronomy, fire detection, biological sensing, and so on.[1,2] Lots of work have been focused on inorganic materials with wide energy band gap such as SiC and GaN.[3–5] However, complex manufacturing processes and high-cost effect hinder the inorganic UV-PDs from further development. Nowadays, a rapid progress of ultraviolet organic photodetectors (UV-OPDs) is made due to their mechanical flexible, lightweight, large-scale power generation, and low cost.[6–8] Both organic small molecules[9–11] and polymers[12,13] are proved to be alternative candidates for UV-OPDs. For instance, highly efficient UV-OPDs with a response of 872 mA/W at −12 V was fabricated based on m-MTDATA and Bphen heterojunction.[14] Also, a solution-processed UV-OPD with a poly(N-vinylcarbazole) PVK:ZnO nanocomposite active layer significantly outperforms the inorganic devices, showing a photocurrent of 70 mA at a wavelength of 360 nm and a maximum responsivity of 1001 A/W.[15] Although PVK is a good candidate for the absorption of UV light due to its wide band gap of 3.4 eV, the charge carrier mobility of 4.8×10^{-9} cm^2/Vs is relatively low leading to low transport efficiency of carriers.[16] Furthermore, the photon absorption of PVK produces short-lived singlet excitons, of which the diffusion length (L_D) is also typically as short as 9.1 nm.[17] Therefore, any attempt from these two aspects can make the device performance further improved.

One promising approach to solve the above problem is adopting long-lived triplet excitons due to their unique properties, including long lifetime, high exciton diffusivity, and high degree of charge transfer.[18,19] Also, phosphorescence materials with triplet excitons are valuable to improve device performances as active layers.[20] However, the effect of phosphorescent iridium complex on UV-OPDs has not yet been extensively studied. In our previous works, an iridium complex of bis[2-(4-tertbutylphenyl) benzothiazolato-N,C2′] iridium (acetylacetonate) [$(t\text{-}bt)_2Ir(acac)$] was widely applied in organic photovoltaic cells[21,22] and organic light-emitting diodes.[23–25] The results showed that $(t\text{-}bt)_2Ir(acac)$ possessed excellent performances with favorable photophysical and electrochemical stability, long exciton lifetime, and potentially long exciton diffusion length. In addition, $(t\text{-}bt)_2Ir(acac)$ displays has stronger ultraviolet absorption than that in visible range, indicating a potential application in fabricating UV-OPDs.

Here, we present an inverted UV-OPD by doping $(t\text{-}bt)_2Ir(acac)$ phosphor into PVK polymer, which was rarely discussed before. The device shows a photoresponse as high as 15.97 A/W under 260 nm UV light. The superior performances of the device resulted from the UV light absorption efficiency, high charge carrier mobility, and the triplet nature of iridium phosphorescent material.

We investigated the effect of $(t\text{-}bt)_2Ir(acac)$ doped in PVK active layer, and the structure of UV-OPDs is ITO/ZnO_x (35 nm)/PVK (120 nm)/MoO_3 (15 nm)/Ag (130 nm) and ITO/ZnO_x (35 nm)/PVK:$(t\text{-}bt)_2Ir(acac)$ (1:10 wt. %, 120 nm)/MoO_3 (15 nm)/Ag (130 nm). The ZnO_x layer was spin coated onto the substrate, followed by annealing at 200 °C in air for 1 h.[26] The active layer was spin-casted on top of ZnO_x layer, and thermally annealed at 80 °C for 30 min. Then, a thin MoO_3 layer and Ag electrode were vacuum deposited subsequently to form a device area of 2 mm^2.

The chemical structures of PVK and $(t\text{-}bt)_2Ir(acac)$, device structure and energy band diagram of UV-OPDs are shown in Figure 1. In the UV-OPDs, ITO and Ag act as the cathode and anode, respectively. Under a negative bias, ZnO_x layer blocks holes from the ITO side in dark condition. When illuminated under 260 nm UV light source with a power of 0.7 mW/cm^2 from Ag side, photogenerated electrons and holes are transported through ZnO_x and MoO_3 layers and collected by ITO and Ag electrodes, respectively.

From UV-Vis absorption spectra in Figure 2(a), there are three absorption peaks of PVK film at 295, 331, and 345 nm. Meanwhile, the absorption spectrum of $(t\text{-}bt)_2Ir(acac)$ film exhibits two peaks at 276 nm and 333 nm. Therefore, the

a)Author to whom correspondence should be addressed. Electronic mail: jsyu@uestc.edu.cn. Tel.: 86-28-83207157.

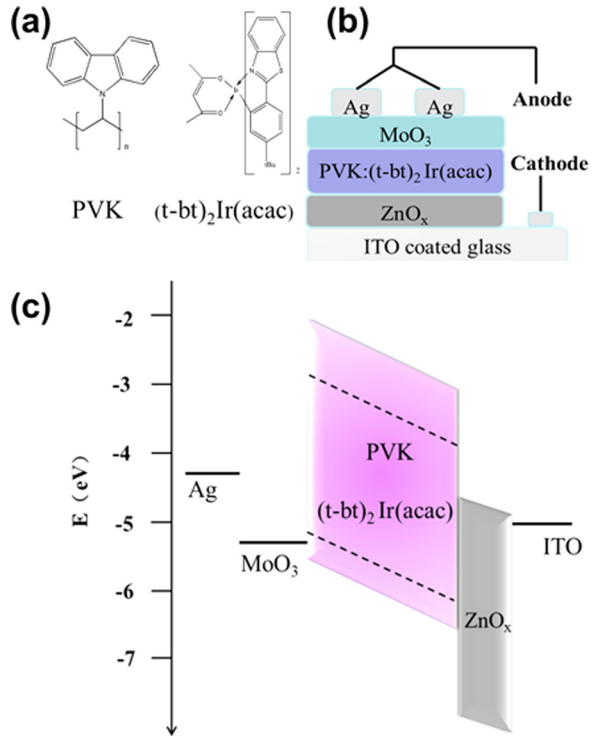

FIG. 1. Chemical structures of PVK and (t-bt)$_2$Ir(acac) (a) and schematic (b) and energy band diagram (c) of UV-OPDs.

active layer mainly has ultraviolet sensitivity ranging from 250 to 350 nm. When doping (t-bt)$_2$Ir(acac) into PVK, the UV absorption becomes stronger, leading to a higher photocurrent particularly in 250–300 nm.

Figure 2(b) displays that the PL peak of PVK is at 425 nm, and those of (t-bt)$_2$Ir(acac) film are at 560 and 600 nm. It is worth noting that the PL density of PVK in the blend film is much weaker than that of (t-bt)$_2$Ir(acac) due to the energy transforming process of excitons from the PVK backbone to (t-bt)$_2$Ir(acac).

The photocurrent density-voltage (J-V) characteristics of UV-OPDs with pure PVK and (t-bt)$_2$Ir(acac) doped PVK layer are displayed in Figure 2(c). Under illumination, the photocurrent of UV-OPDs is enhanced along with increasing reverse bias. At −3 V, the photocurrent density of UV-OPDs without (t-bt)$_2$Ir(acac) is 2.48 mA/cm^2. When doping (t-bt)$_2$Ir(acac) in PVK, 11.37 mA/cm^2 is obtained, which is 4.5 times higher than the control device. It is noted that the photocurrent density under UV light is much higher than that of in dark, indicating that doping (t-bt)$_2$Ir(acac) phosphor into PVK is an effective way to gain high photosensitive characteristic for photodetector. Photoresponse (R) of UV-OPDs is defined by $R = (J_{light} - J_{dark})/P_{in}$, where, J_{light} is the current density under UV illumination, J_{dark} is the dark current density, and P_{in} is the input power of UV light. So the R value of the device with (t-bt)$_2$Ir(acac) doped PVK active layer yields 15.97 A/W at −3 V, which is 381% higher than the undoped, indicating a remarkable improvement for the reported UV-OPDs based on phosphor.[27,28] To further characterize the response speed of our devices, the current density of UV-OPDs as a function of time was recorded at −2 V, as plotted in the inset of Figure 2(c). When UV light applied, current density increases sharply, and decreases to the original value

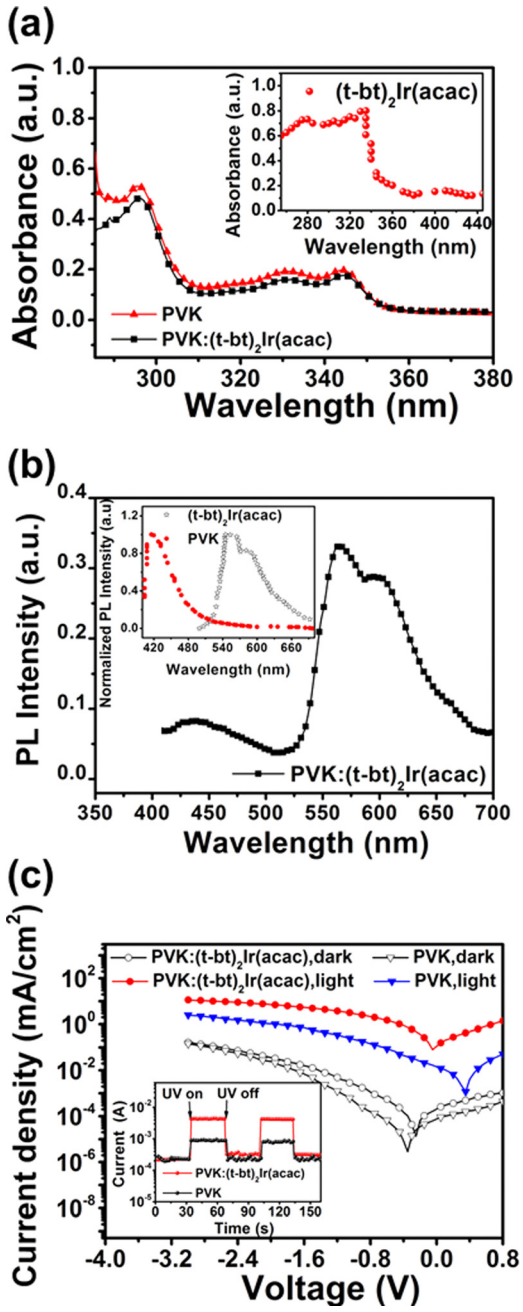

FIG. 2. (a) UV-Vis absorption spectra of PVK and (t-bt)$_2$Ir(acac)/PVK. Inset: UV-Vis absorption spectrum of (t-bt)$_2$Ir(acac). (b) PL spectrum of (t-bt)$_2$Ir(acac)/PVK. Inset: Normalized PL spectra of PVK and (t-bt)$_2$Ir(acac). (c) J-V characteristics of UV-OPDs with and without (t-bt)$_2$Ir(acac) in dark and under illumination. Inset: Photoresponse as a function of time obtained by sudden application and removal of UV light at a bias of −2 V.

instantly upon the removal of light. Both the rise and the fall time are less than 1 s, representing rapid photocurrent response.[28]

Additionally, the detectivity D* can be expressed as $D^* = R/(2qJ_{dark})^{1/2}$, where q is the electron charge. The sensitivity of (t-bt)$_2$Ir(acac) doped device is 6.3×10^{10} cm Hz$^{1/2}$/W at −3 V, comparable to some inorganic UV-PDs.[29] However, despite of the high gain in R, D* is relatively less than the reported UV-OPDs mainly due to the high dark current density. From the energy band diagram in Figure 1(c), we can see that the electron barrier of 1.4 eV between the work function of Ag and the lowest unoccupied molecular

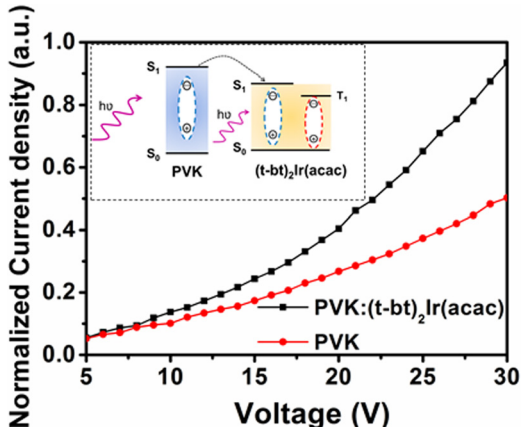

FIG. 3. Normalized J-V characteristics of hole only devices. Inset: Exciton relaxation pathways for $(t\text{-bt})_2Ir(acac)$/PVK systems. S_1 and S_0 are the lowest excited singlet states and singlet ground states, respectively; T_1 is the lowest excited triplet states in $(t\text{-bt})_2Ir(acac)$/PVK system. Blue and red circles are the diffusion of singlet and triplet excitons, respectively.

orbital level of $(t\text{-bt})_2Ir(acac)$ is much lower than the hole barrier of 2.7 eV between the work function of ITO and the valence band of ZnO_x. The high dark current was expected to be from electron injection since MoO_3 layer plays little effect on the electron blocking owing to the deep-lying conduction band edge.[30] Moreover, it reported that the defects and impurities induced during metallic electrode deposition could also cause high dark current. This problem can be solved by improving the electron blocking layer between active layer and electrode.[30–32]

The reasons of high photoresponse for our UV-OPDs can be elucidated from the improved absorption of UV light and enhanced utilization efficiency of excitons. As shown in Figure 2(a), when doping $(t\text{-bt})_2Ir(acac)$ into PVK, $(t\text{-bt})_2Ir(acac)$ phosphor can also absorb the UV light to generate both singlet and triplet excitons, and contribute to the photocurrent. After absorbing the UV light by the PVK layer, short-lived singlet excitons with typically L_D about several nanometers are generated. Since the L_D is much smaller than the thickness ~120 nm of active layer, a large number of excitons are dissipated before transported to the PVK/ZnO_x interface. When doping $(t\text{-bt})_2Ir(acac)$ into PVK (shown in the inset of Figure 3), additional triplet excitons can be obtained from the light absorption of $(t\text{-bt})_2Ir(acac)$ and energy transfer from PVK to $(t\text{-bt})_2Ir(acac)$. As the long exciton lifetime of triplet excitons can effectively suppress the detrimental recombination of hole and electron, triplet excitons of $(t\text{-bt})_2Ir(acac)$ have higher probability to be dissociated into charge carriers than the singlet excitons of PVK.

To further analyze the reason of high photoresponse, we used the hole only carrier method to characterize the charge carrier transportation ability of active layers. It is known as Mott-Gurney laws:[33] $J = -\varepsilon\varepsilon_0\mu V/d$, where ε and ε_0 are the permittivity of the vacuum and polymer, respectively. μ is the charge carrier mobility, and d is the thickness of active layer.[33] Hole only devices were fabricated with a structure of ITO/MoO_3/organic layer/MoO_3/Ag. The normalized J-V characteristics are presented in Figure 3. The hole mobility of $(t\text{-bt})_2Ir(acac)$ doped PVK film is significantly enhanced. Thus, phosphorescent material doped into polymer can improve the hole mobility and transportation of charge carrier.

Moreover, the atomic force microscopy (AFM) height-mode images of PVK films without/with $(t\text{-bt})_2Ir(acac)$ doping are presented in Figures 4(a) and 4(b). It can be seen that a rougher film surface is obtained in the blend film. This change ensures larger contact area and stronger interaction between the active layer and electrode,[34] resulting in a

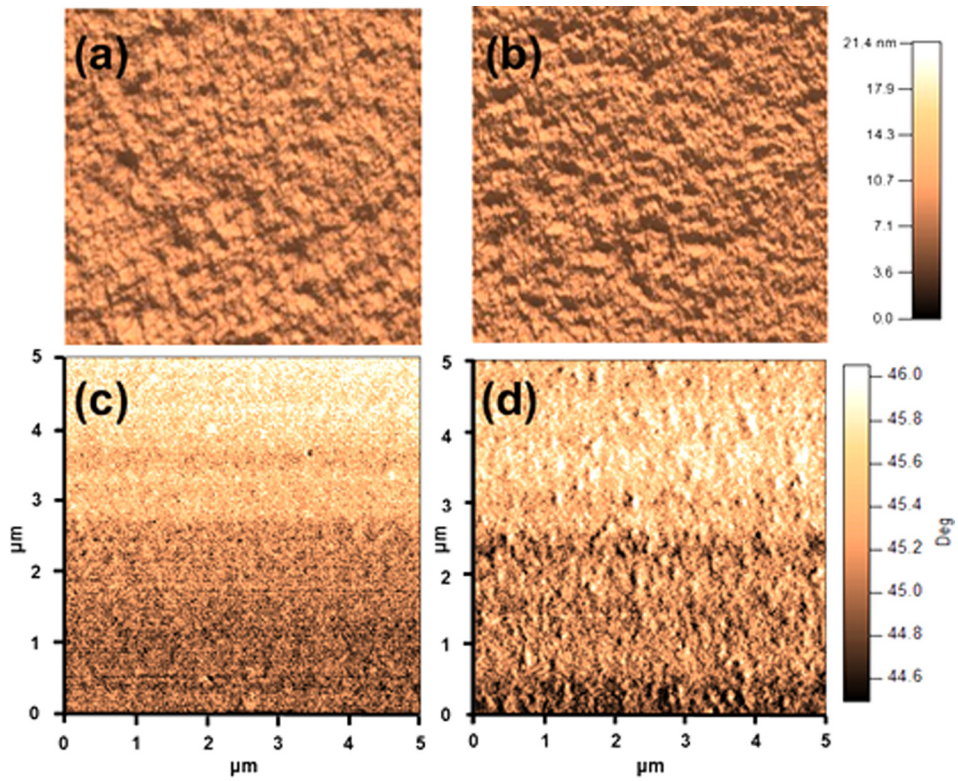

FIG. 4. Tapping-mode AFM images of active layer. Height-images of films without/with $(t\text{-bt})_2Ir(acac)$ in (a) and (b), phase-images of films without/with $(t\text{-bt})_2Ir(acac)$ in (c) and (d), respectively.

higher photocurrent. Furthermore, the rough film surface of $(t\text{-bt})_2$Ir(acac) doped PVK film can also increase light scattering, resulting in the strong absorption of UV light compared with the pristine PVK film. The phase-mode images of PVK films without/with $(t\text{-bt})_2$Ir(acac) are presented in Figures 4(c) and 4(d). Compared with the pristine PVK film, there is an obvious phase separation in $(t\text{-bt})_2$Ir(acac) doped PVK film beneficial for constituting better discontinuous network instead of isolated domains and facilitating charge transporting to electrodes,[26] resulting in higher hole mobility and photocurrent.

We demonstrated a highly efficient inverted UV-OPDs by doping $(t\text{-bt})_2$Ir(acac) phosphor into PVK as the photoactive layer. A high photoresponse of 15.97 A/W under a 260 nm UV light was obtained. The excellent performance of our UV-OPDs is attributed to the strong UV light absorption, the triplet nature of $(t\text{-bt})_2$Ir(acac) phosphor and improved charge carrier transport. It is believed that introducing phosphorescent material with strong ultraviolet absorption is a promising alternative method to improve photoresponse and fabricate low cost UV-OPDs.

This work was supported by the National Science Foundation of China via Grant No. 61177032.

[1]M. Razeghi and A. Rogalski, J. Appl. Phys. **79**, 7433 (1996).
[2]K. J. Baeg, M. Binda, D. Natali, M. Caironi, and Y. Y. Noh, Adv. Mater. **25**, 4267 (2013).
[3]A. Sciuto, F. Roccaforte, and V. Raineri, Appl. Phys. Lett. **92**, 093505 (2008).
[4]Y. Zhang, S. C. Shen, H. J. Kim, S. Choi, J. H. Ryou, R. D. Dupuis, and B. Narayan, Appl. Phys. Lett. **94**, 221109 (2009).
[5]S. R. Forrest, Nature **428**, 911 (2004).
[6]X. Xie, L. Rieth, S. Merugu, P. Tathireddy, and F. Solzbacher, Appl. Phys. Lett. **101**, 93702 (2012).
[7]G. Yu, K. Pakbaz, and A. J. Heeger, Appl. Phys. Lett. **64**, 3422 (1994).
[8]J. Huang, Y. Qi, H. Wang, and J. Yu, Appl. Phys. Lett. **102**, 183302 (2013).
[9]S. H. Wu, W. L. Li, B. Chu, C. S. Lee, Z. S. Su, J. B. Wang, F. Yan, G. Zhang, Z. Z. Hu, and Z. Q. Zhang, Appl. Phys. Lett. **96**, 093302 (2010).
[10]L. Zhu, W. S. Wang, Z. G. Yao, X. Q. Zhang, and Y. S. Wang, Solid State Electron. **80**, 14 (2013).
[11]S. H. Wu, W. L. Li, B. Chu, C. S. Lee, Z. S. Su, J. B. Wang, Q. J. Ren, Z. Z. Hu, and Z. Q. Zhang, Appl. Phys. Lett. **97**, 023306 (2010).
[12]L. Wang, D. Zhao, Z. Su, F. Fang, B. Li, Z. Zhang, D. Shen, and X. Wang, Org. Electron. **11**, 1318 (2010).
[13]H. G. Li, G. Wu, H. Z. Chen, and M. Wang, Curr. Appl. Phys. **11**, 750 (2011).
[14]C. Liu, L. Liu, G. Che, Y. Cui, Q. Wang, W. Li, and M. Liu, Sol. Energy Mater Sol. Cells **96**, 29 (2012).
[15]F. Guo, B. Yang, Y. Yuan, Z. Xiao, Q. Dong, Y. Bi, and J. Huang, Nat. Nanotechnol. **7**, 798 (2012).
[16]P. D'Angelo, M. Barra, A. Cassinese, M. G. Maglione, P. Vacca, C. Minarini, and A. Rubino, Solid State Electron. **51**, 123 (2007).
[17]S. P. Yang, D. Huang, D. Y. Ge, B. Y. Liu, L. S. Wang, and G. S. Fu, Chin. Phys. Lett. **28**, 087101 (2011).
[18]W. Lee, T. H. Kwon, J. Kwon, J. Y. Kim, C. Lee, and J. I. Hong, New J. Chem. **35**, 2557 (2011).
[19]S. Minnikanti, G. Diao, J. J. Pancrazio, X. Xie, L. Rieth, F. Solzbacher, and N. Peixoto, Acta Biomater. **10**, 960 (2014).
[20]Z. Kong, W. Li, G. Che, B. Chu, D. Bi, L. Han, L. Chen, Z. Hu, and Z. Zhang, Appl. Phys. Lett. **89**, 161112 (2006).
[21]J. Huang, J. Yu, W. Wang, and Y. Jiang, Appl. Phys. Lett. **98**, 023301 (2011).
[22]J. Yu, J. Huang, H. Lin, and Y. Jiang, J. Appl. Phys. **108**, 113111 (2010).
[23]J. Zhao, J. Yu, Z. Ma, L. Li, and Y. Jiang, Synth. Met. **161**, 2417 (2011).
[24]J. Zhao, J. Yu, X. Wang, and L. Zhang, Solid State Electron. **81**, 63 (2013).
[25]J. Wang, Y. D. Jiang, J. S. Yu, S. L. Lou, and H. Lin, Appl. Phys. Lett. **91**, 131105 (2007).
[26]X. Liu, H. Wang, T. Yang, W. Zhang, I. F. Hsieh, S. Z. D. Cheng, and X. Gong, Org. Electron. **13**, 2929 (2012).
[27]C. B. Liu, M. Liu, G. B. Che, B. Su, L. Wang, X. X. Zhang, and S. Zhang, Solid State Electron. **89**, 68 (2013).
[28]L. Li, F. Zhang, Q. An, Z. Wang, J. Wang, A. Tang, H. Peng, Z. Xu, and Y. Wang, Opt. Lett. **38**, 3823 (2013).
[29]K. Wang, C. Xue, T. Liang, B. Jiao, W. Zhang, D. Chen, and J. Xiong, J. Infrared, Millimeter, Terahertz Waves **31**, 810 (2010).
[30]D. S. Leem, K. H. Lee, K. B. Park, S. J. Lim, K. S. Kim, Y. W. Jin, and S. Lee, Appl. Phys. Lett. **103**, 043305 (2013).
[31]F. Guo, Z. Xiao, and J. Huang, Adv. Opt. Mater. **1**, 289 (2013).
[32]S. Valouch, C. Hönes, S. W. Kettlitz, N. Christ, H. Do, M. F. G. Klein, H. Kalt, A. Colsmann, and U. Lemmer, Org. Electron. **13**, 2727 (2012).
[33]V. Mihailetchi, J. Wildeman, and P. Blom, Phys. Rev. Lett. **94**, 126602 (2005).
[34]W. Ma, C. Yang, X. Gong, K. Lee, and A. J. Heeger, Adv. Funct. Mater. **15**, 1617 (2005).